



Biomedical applications of carrageenan hydrogel impregnated with zinc oxide nanoparticles

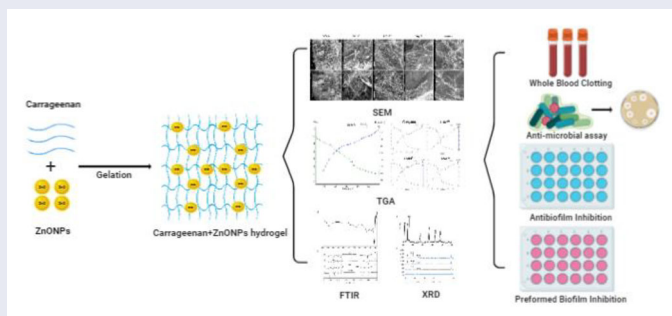
M. Sathish^{a*} , T. Gobinath^{a*}, A. Sundaramanickam^a , K. Saranya^b, A. Nithin^a, and P. Surya^a

^aCentre of Advanced Study in Marine Biology, Annamalai University, Parangipettai, Tamil Nadu, India; ^bCSIR – Central Leather Research Institute (CLRI), Chennai, Tamil Nadu, India

ABSTRACT

Nanotechnology involving biopolymers is comprehensively used in biomedical applications, planning sciences, and food development. The present work describes the synthesis, characterization, and application of carrageenan and zinc oxide nanoparticles (ZnONPs) based hydrogel. The synthesized hydrogels were subsequently characterized using FTIR, XRD, SEM, and TG-DTA. The swelling property, antioxidant activity, and whole blood clotting effectiveness of the Carrageenan hydrogel, and Carrageenan Hydrogels Impregnated with Zinc Oxide Nanoparticles were evaluated. The Carrageenan + ZnONPs (C/ZnONPs) hydrogels showed good antioxidant, and blood clotting activity than the pure carrageenan hydrogel. In addition, the stable C/ZnONPs hydrogels exhibit good antimicrobial activities against both Gram-negative and Gram-positive bacterial strains. Biofilm analysis showed that C/ZnONPs hydrogels have excellent anti-biofilm potential in both inhibition and disruption of preformed biofilm. The obtained results suggested that the carrageenan and Zinc oxide nanoparticles based hydrogel have promising biological applications.

GRAPHICAL ABSTRACT



ARTICLE HISTORY

Received 4 November 2020

Accepted 7 June 2021

KEYWORDS

C/ZnONPs; hydrogel; antibacterial; antibiofilm; wound dressing

Introduction



Pathogenic microorganism resistance to frequently used antibiotic substances have become an important health concern in the 21st century. The development of microorganism resistance to antibiotics has significantly increased morbidity and mortality, longer hospitalization and increased health care costs.^[1] Resistance is increasing against antibiotics, particularly to the first line, inexpensive, and broad-spectrum antibiotics, but also to the newly developed antibiotics; since the development of novel alternative is necessary.^[2,3]

In the specific case of wound management there are several reports of the microorganism resistance to the drug used to manage wounds.^[4] The role of microbial infections in the development of wound infections is well established, the life threatening nature of the wound infections has


maximized its importance in human health. In addition, the cost of medication for wound management is also high.^[5,6] Hence the exploration of new substance for the wound management is very important.

An important factor to take into consideration, when nanoparticles are utilized is how they are move to the site of activity; for this, several methods have been developed like hydrogels, hydrocolloids, alginates, polyurethane foam films, and silicone gels.^[7]

Hydrogel are three dimensional hydrophilic polymeric chains which facilitate mass oxygen transfer.^[8] These hydrogels have several advantageous properties such as high biocompatibility, low immunogenicity and cytotoxicity, ease of functionalization and tunable physicochemical properties which has paved the way toward garnering applications in

CONTACT A. Sundaramanickam  fish_lar@yahoo.com  CAS in Marine Biology, Faculty of Marine Sciences, Annamalai University, Parangipettai, Chidambaram, Tamil Nadu 608502, India.

†These authors contributed equally to this work.

 Supplemental data for this article can be accessed at the [publisher's website](#).

tissue engineering.^[9,10] Other applications of hydrogels include cell transplantation and differentiation, endogenous regeneration, sustained drug delivery, bio prosthetics and wound healing.^[8–11] Polysaccharide based hydrogels prove advantageous over other types of hydrogels owing to their properties such as enhanced biological activity, biocompatibility and biodegradability, mechanical stability as well as scope for chemical modification.^[12]

Hydrogel act as effective wound dressing material owing to their water holding property which keeps the wound moist thereby facilitating rapid cure by means of cell migration and re-epithelialization.^[13] These gels accelerate wound healing process by acting as physical barriers against microbes. Metallic nanoparticles namely zinc oxide (ZnONPs) and Copper oxide (CuONPs) have promising antibacterial activity as demonstrated by previous workers.^[14–16] Hydrogels incorporated with ZnONPs and CuONPs exhibit multifunctional properties.^[17] ZnONPs incorporated hydrogels showed effective antibacterial activity with gram negative than the gram positive bacteria.^[18]

Carrageenan is the sulfated polysaccharides acquired by extraction of red marine algae. It exhibits an effective approach for drug deliverance as a nanoparticle due to its biodegradability, biocompatibility and non-toxicity.^[19] Besides, carrageenan and its modifications has been previously used in controlled drug delivery system, wound dressing and tissue engineering.^[20]

Nanoparticles have been successfully applied in the fluorescent biological labels, bio detection of pathogens, searching of DNA structure, drug and gene delivery, recognition of proteins, tissue engineering, tumor destruction, screening and purification of natural molecules and cells, MRI contrast enhancement, phagokinetic studies.^[21] Zinc Oxide (ZnO) is an essential metal oxide with several potential biological^[22] biomedical^[23,24] wound healing and antimicrobial applications.^[25,26] Especially, zinc oxide nanoparticles (ZnONPs) can be found in numerous industrial products including rubber, pharmaceutical and cosmetic industries, textile industry, electronics and electrotechnology industries, and photocatalysis.^[27–29] In addition, ZnONPs have been examined for their ability to reduce microbial infections in skin and burn wounds.^[30,31] ZnONPs is used in many ointments for the healing of injuries due to its outstanding antimicrobial properties.^[32,33] Currently, it's getting renowned attention due to its unique and potential applications in various fields of research.^[34–36] The various applications are enhanced by nanoparticle interaction with cellular components.^[22,37–42]

The abundantly available polysaccharides such as alginate, agarose, chitosan, etc. have paved way for its usage in tissue engineering applications.^[43–45] Such biopolymers have a simple and effective extraction process that enables large-scale production.

The aggregate of metal nanoparticles and biopolymers has attracted a large attention due to its flawless character for the ideal wound dressing properties.^[46] In the current investigation, we planned to investigate the efficiency of both carrageenan and ZnONPs.

Hence, carrageenan mixed with different concentrations of ZnONPs and hydrogel was for prepared. Nevertheless, in a parallel research done by Oun & Rhim (2017) mixing two ZnO and CuO NPs and prepared the hydrogels.^[17] But, their study was limited to antimicrobial activity of some food pathogens. However, this study we have intended to evaluate many biomedical applications of the carrageenan based nano hydrogels.

The simple extraction process coupled with abundant applications of ZnO based hydrogels have paved the way for us to extend the study toward effective wound healing treatment.

The prepared hydrogel was used in order to evaluate the changes in the properties of the polymer-nanoparticle combinations. The hydrogels were delineated using FTIR, XRD, TG-DTA and SEM. The effects of nanoparticles on the morphology, swelling characteristics of the hydrogel were tested. Antimicrobial and biofilm of the hydrogels was tested on both gram-negative and gram-positive bacteria. Further, the antioxidant activity and blood clotting activities of the synthesized hydrogel were tested.

Materials and methods

Materials

I-Carrageenan, zinc nitrate ($\text{ZnN}_2\text{O}_6 \cdot 6\text{H}_2\text{O}$), Sodium hydroxide pellets (NaOH), Potassium chloride (KCl), and Glycerol ($\text{C}_3\text{H}_8\text{O}_3$) Himedia, India, were used without any further purifications.

Synthesis of ZnONPs

ZnONPs were prepared by reducing $\text{ZnN}_2\text{O}_6 \cdot 6\text{H}_2\text{O}$ using NaOH as a reducing agent. 29.75 g (0.1 M) $\text{ZnN}_2\text{O}_6 \cdot 6\text{H}_2\text{O}$ was dissolved in 1000 ml of double distilled water with stirring for 30 min and heated to boil. Then 60 ml of 5 M NaOH solution was added drop wise to the $\text{ZnN}_2\text{O}_6 \cdot 6\text{H}_2\text{O}$ solution and incubate at 80 °C for 2 h. The white precipitate indicates the formation of ZnONPs, the precipitate was washed three times with distilled water and three times with absolute ethanol, and then it was desiccated in an oven at 70 °C for 6 h. The ZnONPs were kept in air tight container until further use.^[17]

Synthesis of carrageenan based hydrogels

Three grams of carrageenan was completely dissolved into 150 ml of distilled water with 0.9 g of glycerol as a plasticizer. Prepared solution was heated at 90 °C for 20 min, then 2.5 ml of 1 M KCl solution was poured to initiate gelation process.^[17] Three different concentrations of Carrageenan + ZnONPs (C/ZnONPs) hydrogels were prepared with of ZnONPs (1 wt % of carrageenan, 2 wt % of carrageenan, and 3 wt % of carrageenan). For hydrogel preparation, ZnONPs were added to 150 ml of distilled water and placed in one for 4 hours for uniform distribution. 3 g, of carrageenan 0.9 g glycerol and 2.5 ml KCl were added to

the solution according to the same protocol as mentioned earlier.

Morphological analysis (SEM)

The structure of carrageenan and C/ZnONPs hydrogel was observed using a scanning electron microscope (JEOL-JSM 5610LV, JEOL, Ltd, Tokyo, Japan) at an acceleration voltage of 10 kV and a current of 10 mA after sputter coating the samples with gold.

Categorization of hydrogels

FTIR and XRD analysis of hydrogels

The chemical arrangement of the prepared hydrogels was evaluated using FTIR spectra, for this, freeze dried carrageenan based hydrogels were placed on the stage and spectra was recorded in the range of 4000–400 cm^{-1} .

The X-ray diffraction patterns of hydrogels were analyzed by XRD diffractometer. Hydrogels was placed on a glass slide and the spectra were recorded using Cu $K\alpha$ radiation at a wavelength of 0.154 nm and a monochromator filtering wave at 40 kV and 30 mA.

The diffraction pattern was obtained at diffraction angles between $2\theta = 30\text{--}80^\circ$ with a scanning speed of $0.4^\circ/\text{min}$ at room temperature.

Thermal properties

Temperature stability of hydrogels was analyzed by a simultaneous thermal analyzer (NETZSCH-STA 449 F3 JUPITER Instrument, Germany). The measured amount of hydrogel samples were heated in the temperature ranged from 30 to 600°C with a heating range of $20^\circ\text{C}/\text{min}$ under a nitrogen stream of $50 \text{ cm}^3/\text{min}$.

Swelling ratio

To establish swelling ratio (SR) for the hydrogels, pre-weighed freeze dried hydrogels were immersed in swelling medium. After incubation of samples, the surface water were removed and weighed. The swelling ratio was calculated as follows.

$$\text{SR} = (\text{W}_2 - \text{W}_1)/\text{W}_1$$

Here, SR is the swelling ratio, W_1 is the weight before swelling and W_2 is the weight after swelling.^[47]

Release study of ZnONPs from hydrogels

The UV-Vis absorption spectra of ZnONPs from the hydrogels were recorded by using UV-Vis spectrophotometer. About 5 mg of freeze dried hydrogel disks were immersed in 5 ml of distilled water and incubate at room temperature. The medium ($\sim 3 \text{ ml}$) was transferred into a quartz cell and absorbance was recorded in the wavelength range 300–700 nm.^[48]

DPPH

The antioxidant assay was estimated utilizing DPPH (2,2-diphenyl-2-picrylhydrazyl hydrate) according to the method described by Nagaich and Gulati.^[49] A stock solution of DPPH was prepared in ethanol; 1 ml of this solution was poured into 3 ml of hydrogel extract (1 g of hydrogel in 10 ml of distilled water). The blend was stunned and allowed to incubate at room temperature for 30 min. Then the absorbance was determined at 517 nm by using a UV-Vis spectrophotometer. Antioxidant activity was estimated as follows.

$$\begin{aligned} \% \text{ Inhibition} &= (\text{control absorbance} \\ &\quad - \text{sample absorbance}/\text{control absorbance}) \\ &\quad \times 100 \end{aligned}$$

Whole blood clotting assay

Whole blood clotting study of the hydrogels was performed according to the method described by Liu^[50] with minor modifications. Blood was drawn out from healthy volunteers in anticoagulant tubes. 200 μl of blood was added to 10 mg freeze dried hydrogels and was placed in a 24 well plate, further 0.1 M CaCl_2 was added to initiate blood clotting. Hydrogels were incubated at 37°C for 10 min. After incubation 2 ml distilled water was added drop wise without disturbing the clot. Subsequently, 1 ml of solution was taken and centrifuged at 1000 rpm for 1 min. Supernatants were collected for each sample and maintained at 37°C for 1 h then 200 μl of this solution was transferred to a 96 well plate and then measured at 540 nm with ELISA reader.

Microbial studies

Antimicrobial assay

The antibacterial assay of hydrogels was evaluated by using the agar diffusion method against the gram-negative and the gram-positive bacteria. Briefly, 100 μl of bacterial suspension was spread out on the agar surface. Further, the hydrogels were added into the wells, the petri dishes were incubated for 12 h at 37°C . Zones of inhibition were evaluated by calculating diameter of the bacterial growth inhibition zone around the wells.^[51]

Disruption of preformed biofilm

The antibiofilm efficacy of hydrogels on biofilm formation by Gram-positive bacteria such as *Bacillus subtilis*, *Staphylococcus aureus* and Gram-negative bacteria *Escherichia coli*, *Klebsiella pneumoniae* bacteria were examined by following the protocol described by^[52] with minor changes. All bacterial strains were purchased from Raja Muthiah Medical College, Chidambaram, Tamilnadu, India. The bacterial suspensions were added into 24 well culture plates. To ensure the proper biofilm formation of cultured plate was incubated at 37°C for 24 h. After incubation, non-adhesive cells were removed and washed with

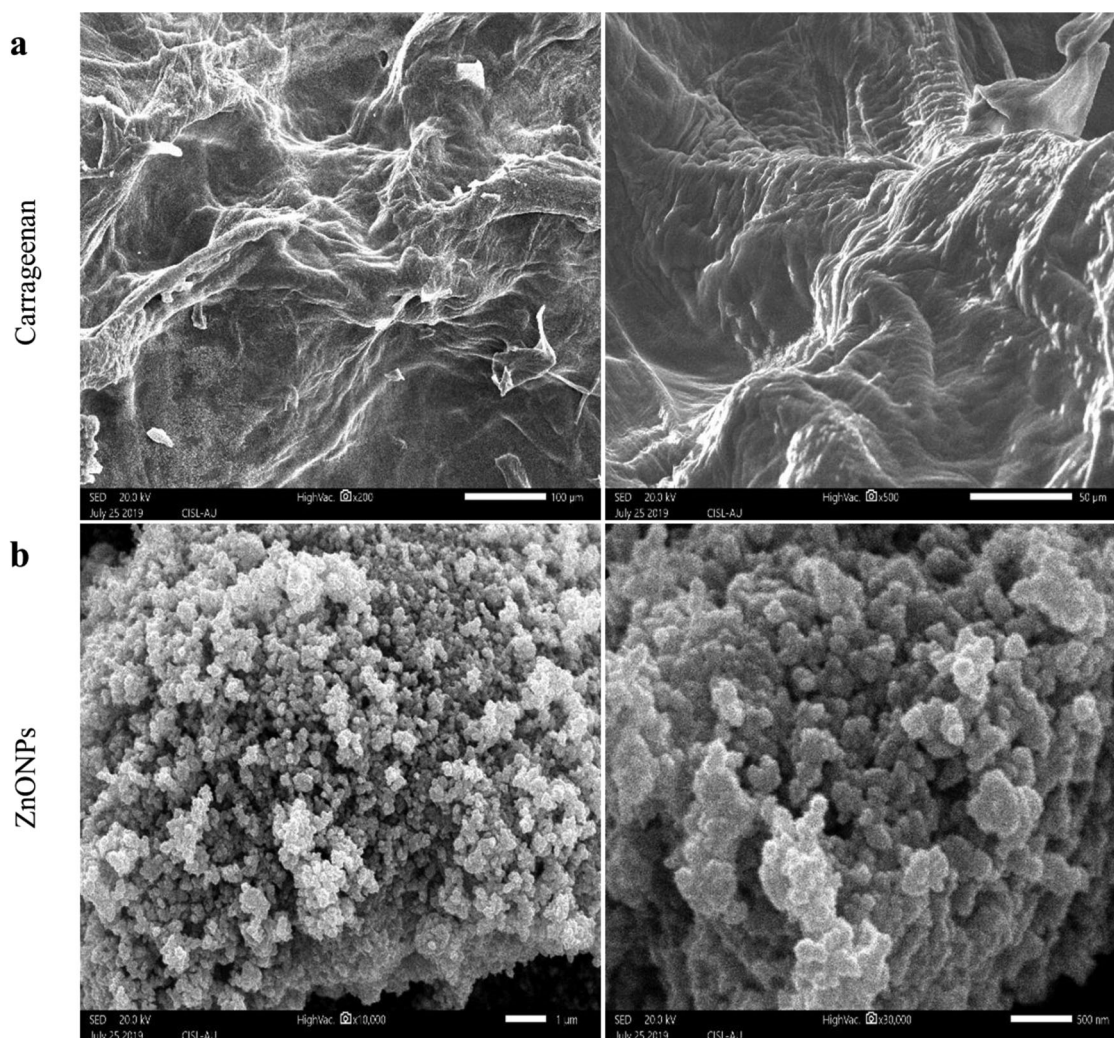


Figure 1. (A) SEM images at different magnification micrographs of Carrageenan and SEM ZnONPs. (B) SEM images at different magnification micrographs of C/ZnO^{1%}, C/ZnO^{2%}, and C/ZnO^{3%}.

sterile phosphate buffered saline (PBS). For the control, biofilms were treated with 0.1 g of hydrogels sample for 24 h at 37 °C. Untreated wells were incubated with 100 μ l sterile distilled water. After 24 h, media was removed and formed biofilms was then fixed with 100 μ l absolute methanol. The plates were kept incubated for 15 min at 37 °C. Methanol was removed from the plate and biofilms were briefly stained with 0.1% crystal violet and incubated for 30 min at room temperature. Excess strains were thoroughly removed with distilled water and then plates were left to dry for 5 h. After drying, 20% glacial acetic acid was poured to each well. De-stained solution was further transferred into 96 well plates then optical density was measured at 595 nm with ELISA reader.

Biofilm inhibition

This assay traditionally used to estimate the drug efficacy to prevent biofilm formation. For test wells, 0.1 g of hydrogels was added to plate and seeded with bacterial suspension, untreated wells incubated with 100 μ l of sterile distilled water and kept incubated at 37 °C for 24 h. After incubation, biofilms inhibition was assessed by the violet stain as described in 2.8.2.

Result and discussion

Morphological analysis

General observation

The transformation of liquid hydrogels into solid gel was noticed with the presence of KCl ([supplementary Figure S1](#)). Regardless of ZnONPs concentration, the gelation time of carrageenan based hydrogels was less than 2 min. The fast gelation in this carrageenan-based hydrogels preparation may be advantageous to prevent unwanted diffusion and loss of the delivered species.^[53]

SEM analysis

SEM imaging is one of the promising methods for the topographic analysis of synthesized hydrogels and nanoparticles. SEM images of hydrogels and nanoparticles are shown in [Figure 1A and B](#). Carrageenan was completely dissolved and complete smooth uniform layer was obtained. The incorporation of ZnONPs onto the carrageenan hydrogels was also analyzed through SEM. Vigorous mixing causes ZnONPs dispersed uniformly inside the carrageenan based hydrogels. The homogeneity

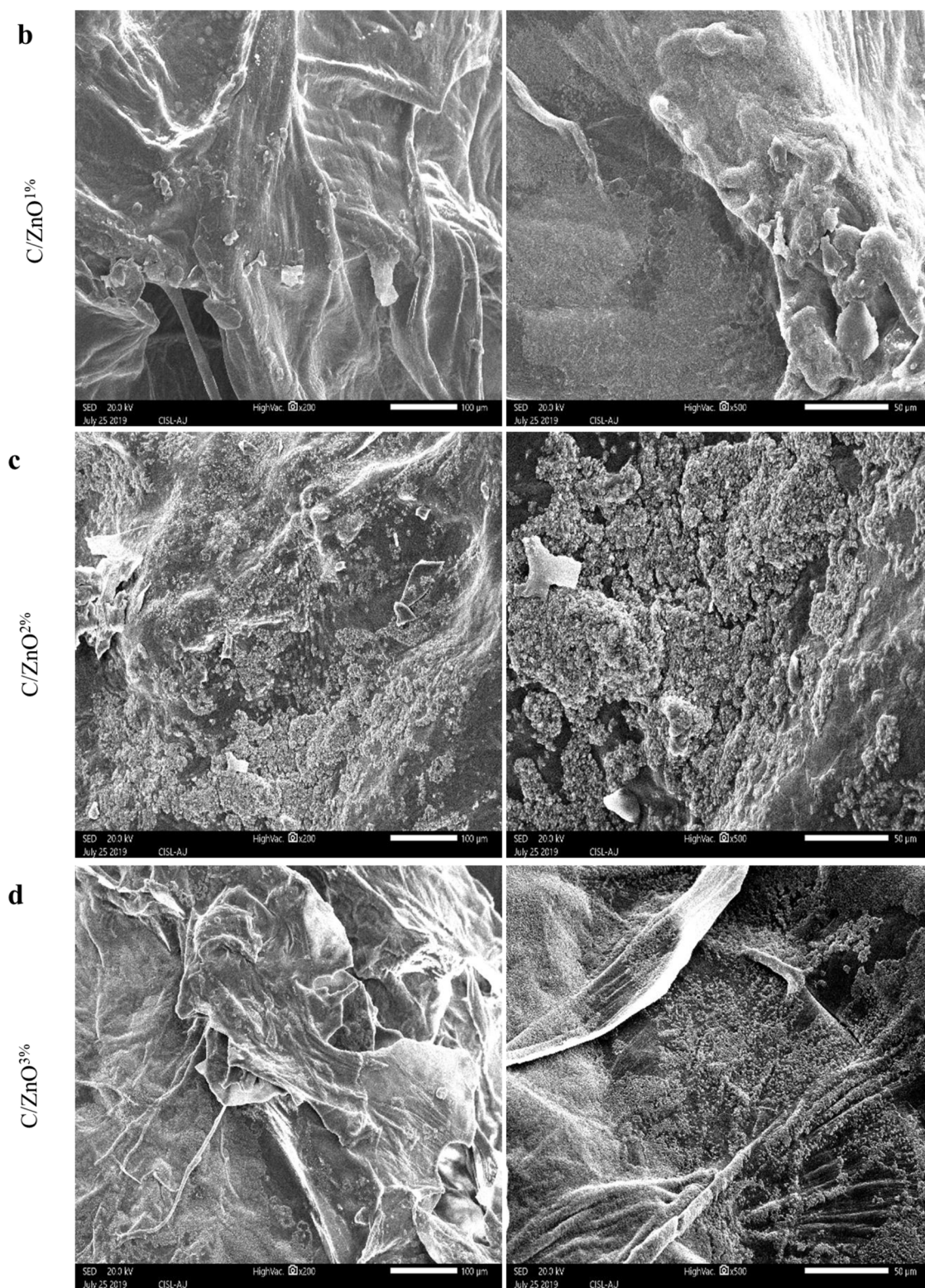


Figure 1. Continued.

and uniform distribution of ZnONPs on the hydrogel matrix are confirmed from this image. C/ZnO^{1%}, C/ZnO^{2%}, and C/ZnO^{3%} hydrogels showed an increased surface roughness with enhancement in the concentrations of ZnONPs. Further, the morphology of ZnONPs was confirmed through SEM analysis and the observed shape of ZnONPs was spherical.

Characterization of ZnONPs and carrageenan based hydrogels

FT-IR

Chemical interactions between carrageenan and ZnONPs were examined by FT-IR spectroscopy, and the observed results are presented in Figure 2. The peaks at 3294 to

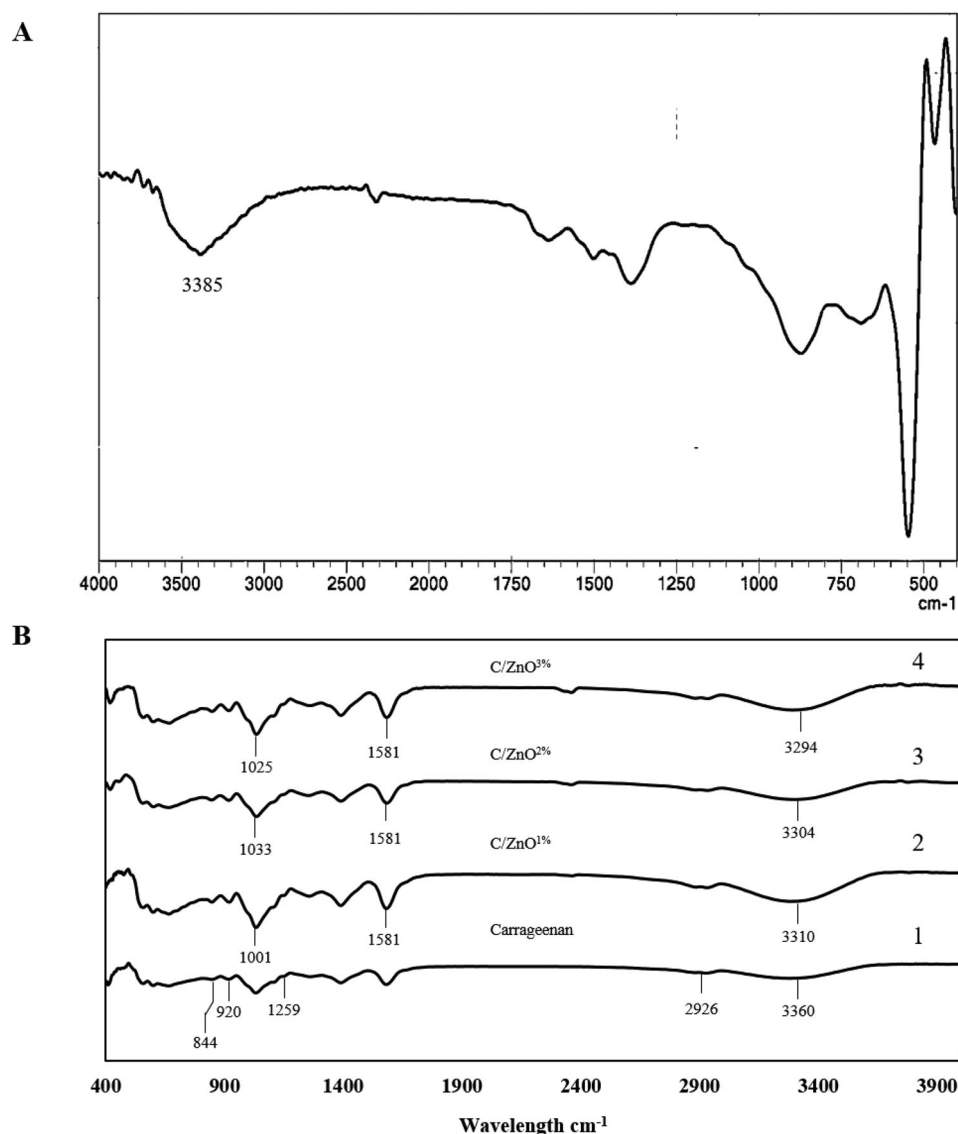


Figure 2. FT-IR spectra of (A) ZnONPs, and (B) (1) Carrageenan hydrogels, (2) C/ZnO^{1%}, (3) C/ZnO^{2%} and (4) C/ZnO^{3%}.

3360 cm⁻¹ were recognized to the stretching of hydroxyl groups. The sharp peak at 2926 cm⁻¹ was matching to the stretching of C-H bonds. The peak at 1581 cm⁻¹ was due to the presence of water molecule. The absorption band at 1259 cm⁻¹ was corresponding to the sulfate ester group. The peaks at 920 and 844 cm⁻¹ were attributed to C-O of 3, 6-anhydro-D-galactose and C-O-SO₃ of D-galactose-4-sulfate. Variations in intensity and peak positions were noticed after integration of nanoparticles, which was corresponding to the interactions between carrageenan and ZnONPs. Similar observations were reported by Oun et al.^[17]

X-ray diffraction

X-ray diffraction (XRD) patterns of the hydrogels are presented in Figure 3. The XRD pattern of the ZnONPs shows the characteristic peaks located at 2θ of 31.8, 34.4, 36.2, 47.65, 56.6, 62.85, 68.08 and 69.09 corresponding to the zinc oxide.^[17,54] The carrageenan hydrogel showed specific diffraction at 2θ of 40.6 and 50.2 representing KCl. The present intensity of C/ZnONPs hydrogel was changes due to

the presence of KCl in hydrogels. ZnONPs added hydrogels exhibits peaks at 2θ of 38.3 and 46.12 corresponding to ZnONPs.

TG-DTA

Thermogravimetric studies of the hydrogels and ZnONPs were conducted from 30 to 600 °C. The TGA and DTA curves for the hydrogels and nanoparticles are shown in Figure 4. No considerable weight loss is observed after this up to 600 °C. The observed results elucidated that ZnONPs is stable even above 398 °C. The weight loss curve of the control carrageenan hydrogel in the range of 260–300 °C are associated with decomposition of carrageenan films.^[17] The corresponding weight loss curves of the C/ZnONPs hydrogels in the range 260–300 °C, suggest the comparable weight loss events of C/ZnONPs hydrogels. TG-DTA analysis shows a loss of 5% up to 398 °C (Figure 4). The residual weight of the carrageenan hydrogel and C/ZnO^{1%}, C/ZnO^{2%} and C/ZnO^{3%} hydrogels were 36.13, 33.27, 36.22, and 38.32 respectively (Table.1).

It was observed that the residual weight of the C/ZnONPs hydrogels varies based on the ZnONPs concentration. C/ZnO^{2%} and C/ZnO^{3%} hydrogels are more stable than carrageenan hydrogel. Among all, C/ZnO^{3%} has more residual weight after TGA thus considered to be the more stable hydrogel in this investigation.

Swelling capability

The swelling capability of hydrogel is used for the measurement of water holding capacity of the C/ZnONPs hydrogels. The swelling capability of carrageenan hydrogel and C/ZnONPs hydrogels increased quickly in the first 10 min of immersion into PBS and the swelling capacity started to decrease after 30 min of immersion. Reduction in the swelling capacity after 30 min was mainly because of the dissolution of carrageenan into the PBS. The carrageenan

hydrogel exhibited the swelling capacity of 2136%, using KCl as cross linker in hydrogel synthesis increased swelling capacity of carrageenan hydrogel in dramatic level. The C/ZnO^{1%}, C/ZnO^{2%}, and C/ZnO^{3%} hydrogels exhibited the swelling capacity of 2563%, 2824% and 3216%, respectively. The increase in the C/ZnONPs hydrogels swelling capacity is dependent on the ratio of cross linker (KCl) and concentration of ZnONPs present in the hydrogels. Incorporation of ZnONPs into carrageenan hydrogels was probably caused by increase mechanical properties to maintain the structural integrity of hydrogels during absorbing PBS. This increase in the swelling capacity has been noticed when carrageenan hydrogel films integrated with ZnONPs and CuONPs.^[17]

Release study of ZnONPs from hydrogels

To understand the ZnONPs release from the carrageenan based hydrogels, in-vitro studies were carried out in pH 7.4 PBS buffer solution at 37 °C. The presence of ZnONPs in the hydrogel was confirmed by UV- Vis spectroscopy. **Supplementary Figure S2** displays the release profile of ZnONPs from C/ZnO^{1%}, C/ZnO^{2%}, and C/ZnO^{3%} hydrogels in 7.4 pH media with respect to time. A distinct absorption maximum is observed at wavelengths 300 nm for the C/ZnO^{1%}, C/ZnO^{2%}, and C/ZnO^{3%} hydrogels respectively. Similar absorption peaks have been reported for zinc oxide nanoparticles.^[55] C/ZnO^{3%} hydrogel have higher release, whereas C/ZnO^{1%} hydrogel has shown less release, this is because of the presence of more ZnONPs that are entrapped inside the hydrogels.^[56]

DPPH radical scavenging activity

The supplementary image (Figure S3) shows the DPPH radical scavenging activity of the carrageenan, C/ZnO^{1%}, C/

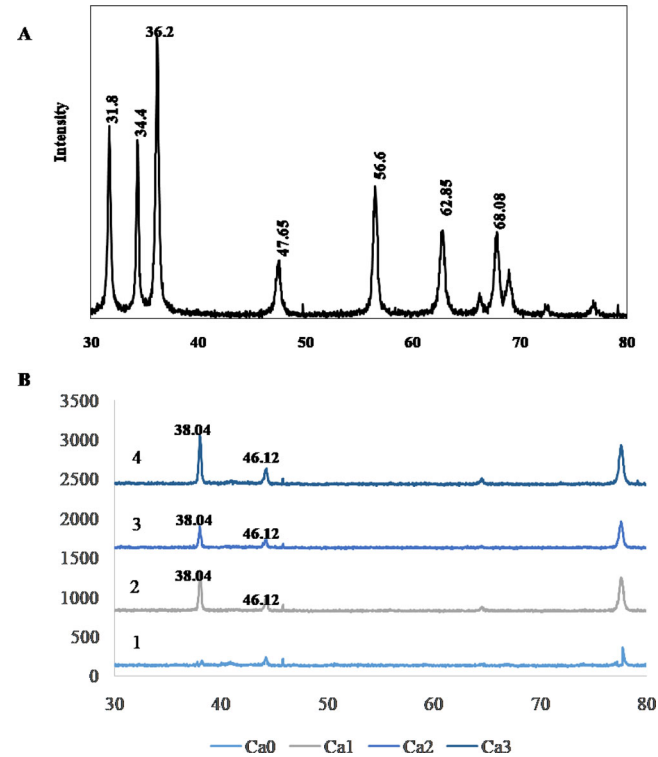


Figure 3. XRD patterns of a (A) ZnONPs, and (B) (1) Carrageenan hydrogels, (2) C/ZnO^{1%}, (3) C/ZnO^{2%} and (4) C/ZnO^{3%}.

Table 1. TG-DTA analysis of carrageenan, C/ZnO^{1%}, C/ZnO^{2%}, C/ZnO^{3%}, and ZnONPs.

| Sample | Residual weight (%) | | |
|----------------------|---------------------|--------|--------|
| | 200 °C | 400 °C | 600 °C |
| carrageenan | 85.24 | 42.23 | 36.13 |
| Ca/ZnO ^{1%} | 87.94 | 43.64 | 38.32 |
| Ca/ZnO ^{2%} | 84.32 | 42.19 | 36.22 |
| Ca/ZnO ^{3%} | 84.55 | 35.03 | 33.27 |
| ZnONPs. | 98.18 | 95.74 | 94.95 |

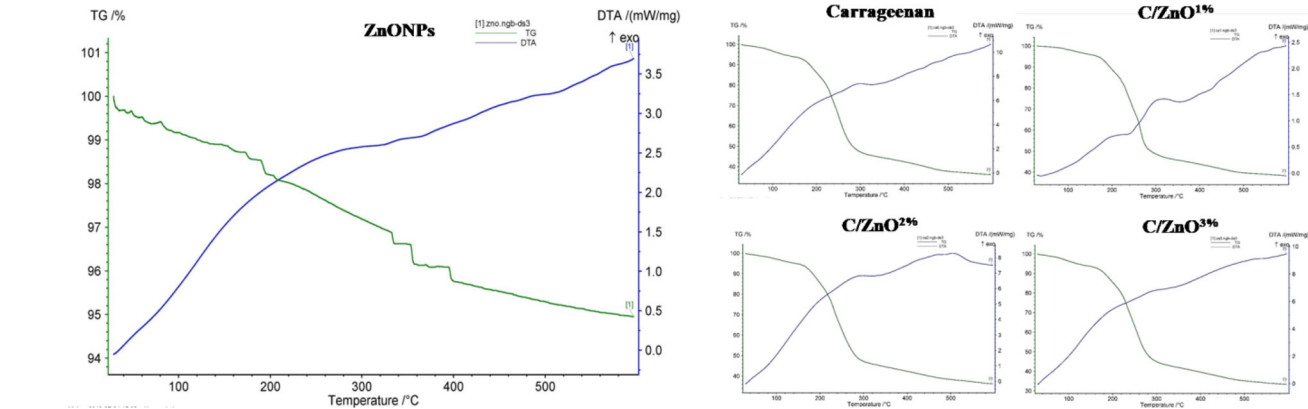


Figure 4. TGA and DTA curves for ZnONPs, Carrageenan, C/ZnO^{1%}, C/ZnO^{2%}, and C/ZnO^{3%} hydrogels respectively.

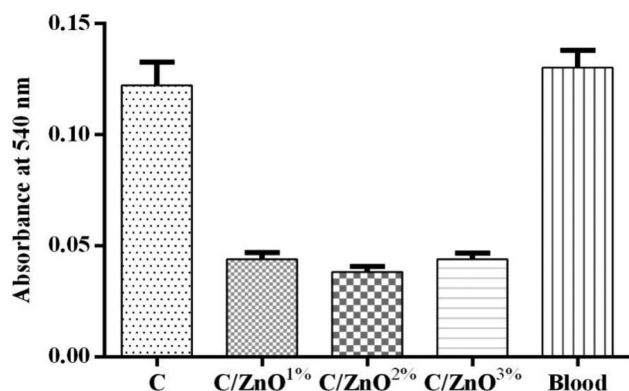


Figure 5. Whole blood clotting evaluation of the carrageenan hydrogel and carrageenan + ZnONPs hydrogels.

ZnO^{2%}, and C/ZnO^{3%} hydrogels. The activity was high and it subsequently decreased with the integration of ZnONPs in the carrageenan hydrogel. The decrease in the antioxidant activity of C/ZnO^{1%}, C/ZnO^{2%}, and C/ZnO^{3%} hydrogels can be explained by many answers. Precisely, the low antioxidant activity was due to the slower release of the ZnONPs from hydrogels. The scavenging activity of the test hydrogel was carrageenan hydrogel > C/ZnO^{1%} > C/ZnO^{2%} > C/ZnO^{3%}. Current study results are consistent with the previous work.^[57]

Whole blood clotting

To evaluate the influence of ZnONPs on the whole blood clotting behavior of carrageenan hydrogels, whole blood was kept in contact with prepared hydrogels.

For comparison carrageenan hydrogel without ZnONPs was selected as control (Figure 5).

The appearance and graphical representation of influence of C/ZnONPs hydrogels on the whole blood clotting behavior is shown in Figures 5 and S4. C/ZnONPs hydrogels have much higher blood clotting efficiency as compared with pure carrageenan hydrogel. When blood was introduced onto the hydrogels, it was rapidly absorbed by the C/ZnONPs hydrogels. However, for the pure carrageenan hydrogels, blood was not absorbed rapidly (Figure S4, A3). To quantify the blood clotting efficiency of hydrogels, blood which is not trapped in the hydrogels was washed away with saline and optical density of the solution was measured (Figure S4, A4). All the C/ZnONPs hydrogels show a decrease in the absorbance value when compared with control thus indicates a faster clotting performance. The existence of ZnONPs in the hydrogels did not alter the blood clotting nature of the carrageenan. However, in a similar research, adding a chitosan hydrogel + Nano ZnO composite has good effects on blood clotting.^[58] Incorporation of ZnONPs into carrageenan hydrogel can lead to more than 50% decrease in the absorbance value of hemoglobin solution. Therefore, C/ZnONPs hydrogels are superior in view of whole blood clotting (Figure 5). Carrageenan is a highly sulfated blood clotting material and also called as good hemostatic agent,^[59] carrageenan blood clotting ability can be attributed to the negatively charged surfaces in the

carrageenan activating factor XII which initiates the inherent pathway of blood coagulation.^[60] C/ZnONPs hydrogels possess in high absorption ability. Due to the connections between the blood and C/ZnONPs hydrogels, the hydrogels could trap more blood leading to more rapid and stable blood clotting compared with pure carrageenan.

Microbial studies

Antimicrobial assays

Antibacterial activity against *B. subtilis*, *S. aureus*, *E. coli* and *K. pneumonia* of the carrageenan, C/ZnO^{1%}, C/ZnO^{2%}, C/ZnO^{3%} hydrogels and ZnONPs was evaluated using agar well diffusion method, and the respective results were presented in Figure 6. The carrageenan hydrogel did not show any antibacterial activity against above mentioned bacteria (Figure S5), but the C/ZnO^{1%}, C/ZnO^{2%}, C/ZnO^{3%} hydrogels and ZnONPs exhibited strong antibacterial activity against all the strains. However, the antibacterial activity was dependent not only on the concentration of ZnONPs but also on the type of bacteria. C/ZnO^{1%}, C/ZnO^{2%}, C/ZnO^{3%} hydrogels and ZnONPs exhibited strong antibacterial activity against Gram-negative bacteria *E. coli* and *K. pneumonia* and Gram-positive *B. subtilis*, and *S. aureus* (Figure 6). Shi et al. and Oun and Rhim also found that the ZnONPs showed stronger antibacterial activity against food pathogens of both Gram-positive and Gram-negative bacteria.^[17,61] The mechanism behind the antibacterial activity of ZnONPs might be due to several reasons such as reactive oxygen species (ROS) generation, zinc ions (Zn²⁺) release, different probable mechanisms.^[61,62] They concluded that the hydrogels releases the entrapped ZnONPs in the surrounding medium thus destroying the microorganisms.

Inhibition of development of pre-formed biofilms

The antibiofilm efficacy of the hydrogels was evaluated against both Gram-negative and Gram-positive bacteria. A standard crystal violet assay for biofilm analysis indicated that hydrogels are effective in eradication of preformed biofilm built by Gram-positive Bacteria i.e., *B. subtilis* and *S. aureus*. Similar results were also noticed in case of biofilm built by Gram-negative *E. coli* and *K. pneumonia*. Besides, an equal amount of carrageenan hydrogel was added to biofilm, and shows significant difference in the ability to disturb preformed biofilm was observed between carrageenan hydrogel and C/ZnONPs hydrogels Figure 7A. which is in consistent with the earlier findings indicating enhancement of biofilm activity of carrageenan.^[63] Thus, the enhanced activity of carrageenan hydrogels could unmistakably be associated to the presence of ZnONPs in hydrogels. Quantification of biofilm indicated that C/ZnONPs hydrogels especially C/ZnO^{2%} and C/ZnO^{3%} were superior to inhibit the biofilm formation of both Gram-negative and Gram-positive. Taken together, these observations established that C/ZnONPs hydrogels were more effectual to disrupt preformed biofilms, regardless of Gram-positive and Gram-negative bacteria.

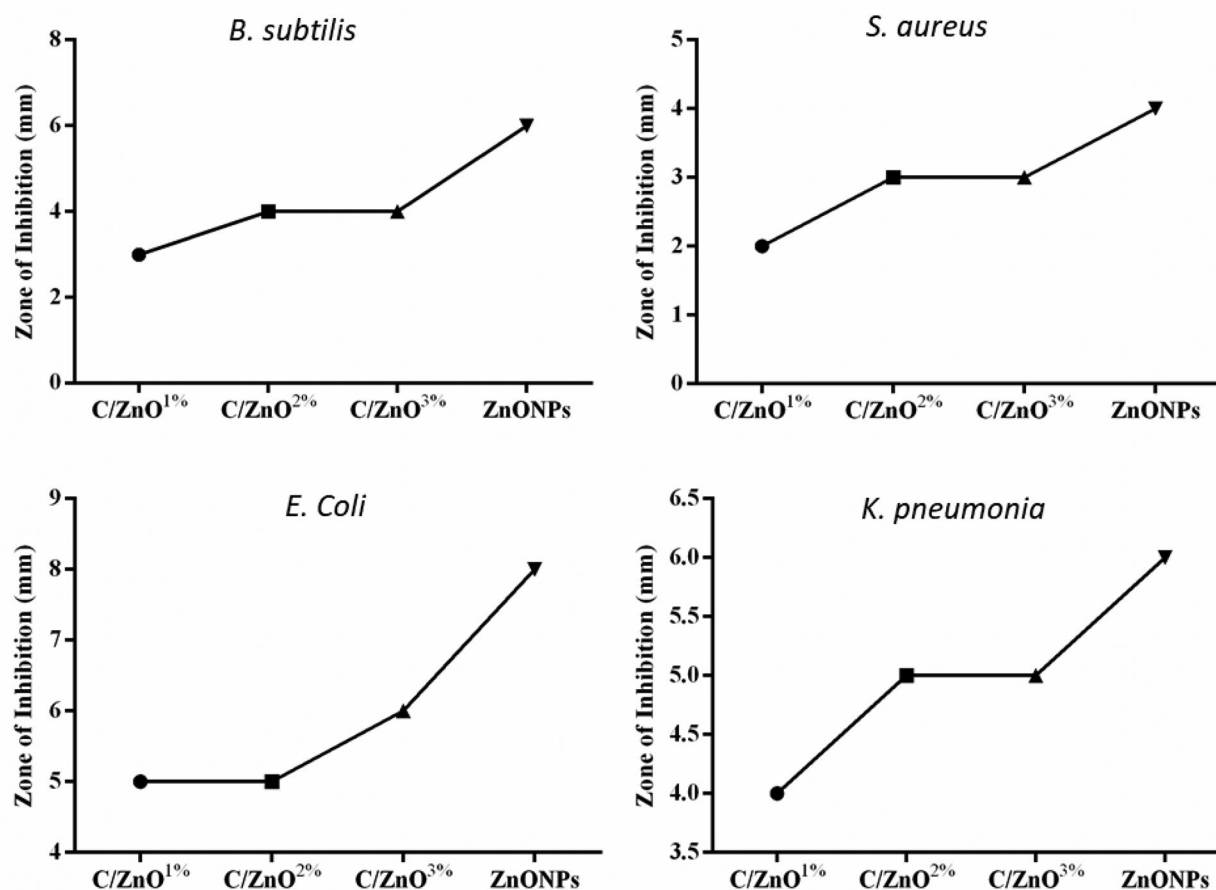


Figure 6. Zone of inhibition evaluations of respective stains *B. subtilis*, *S. aureus*, *E. coli* and *K. pneumonia* against of (1) Carrageenan, (2) C/ZnO^{1%}, (3) C/ZnO^{2%}, (4) C/ZnO^{3%} hydrogels, (5) ZnONPs.

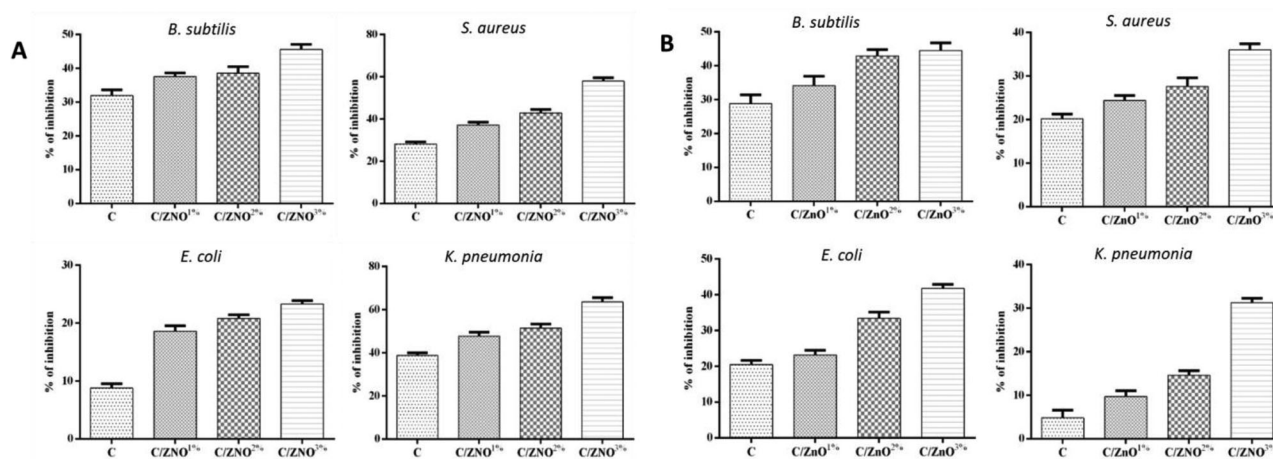


Figure 7. Images of the percentage of (A) pre-formed biofilm and (B) biofilm disrupted by different hydrogel formulations *B. subtilis*, *S. aureus*, *E. coli* and *K. pneumonia*.

Antibiofilm inhibition

Synthesized hydrogels have utilized to inhibit the biofilm activity. In the present study, biofilm inhibition activity of hydrogel was determined with most strong biofilm forming and frequent wound infecting pathogens *B. subtilis*, *S. aureus*, *E. coli* and *K. pneumonia* (Figure 7B). These results indicated that, hydrogels inhibited the biofilm formation of all tested bacterial strains as compared with negative control.

Interestingly, an inhibition of biofilm activity was on concentration based. As a result, *B. subtilis* was inhibited over $45\% \pm 1.26\%$ only by C/ZnO^{3%} hydrogel, while Carrageenan, C/ZnO^{1%}, C/ZnO^{2%} had an inhibition $28\% \pm 1.49\%$, $34\% \pm 1.6\%$, and $45\% \pm 1.06\%$ respectively. The C/ZnO^{3%} hydrogel was shown inhibition up to $36\% \pm 0.8\%$ the biofilm formation of *S. aureus*, other hydrogels have very mild effects on *S. aureus* biofilm formation. In Gram-negative *E.*

coli, biofilm inhibition was shown up to $40\% \pm 0.64\%$, C/ZnO^{3%} hydrogel was the most active. Results with the *K. Pneumonia*, shown as C/ZnO^{3%} hydrogel had significant level of inhibition up to $30\% \pm 0.56\%$. Carrageenan, C/ZnO^{1%}, C/ZnO^{2%} hydrogels did not show significant effectiveness.

The efficacy of disruption preformed biofilm and biofilm inhibition by carrageenan hydrogel and C/ZnONPs hydrogels in vitro analysis was originally demonstrated. Although, *S. aureus*, *E. Coli*, *B. subtilis* and *K. pneumonia* are the common bacterial species frequently identified from wound infections.^[64] All these bacterial pathogens have been increasingly associated with wound infections. If effective measures are not taken for the wound infection the small wound may lead to death.^[65] Recently,^[66–69] demonstrated zinc oxide shows significant biofilm activity against *S. aureus*, *E. Coli*, *B. subtilis* and *K. pneumonia*. Our *in vitro* results were also quite promising, suggesting the hydrogel reinforced with ZnONPs exhibited significant biofilm activity. Thus, C/ZnONPs hydrogels represents a promising composite for the management for bacterial infections and a serious candidate for wound healing applications. The release of Zn ion from ZnONPs will be checked in our future work.

Conclusion

The synthesized C/ZnONPs hydrogels was produced by a simple and efficient method, performing proper swelling capacity and much better mechanical properties. It exhibited better antioxidant, blood clotting activity and also possess excellent antibacterial and biofilm efficacy against *B. subtilis*, *S. aureus*, *E. coli* and *K. pneumonia*. The present study confirmed that C/ZnONPs hydrogel have multi-potential property. Thus, the present study suggests that this bio-reduction practice is a well suitable system for large-scale production. The blood clotting and biofilm efficacy were tested in this study only at the grassroot stage which needs to be addressed further.

Acknowledgements

The authors acknowledge authorities of Annamalai University for providing necessary facilities.

Conflict of interest

There is no conflict of interest between the authors.

Funding

This study was supported by a research grant from Ministry of Earth Sciences (MoES), National Centre for Coastal Research, Government of India (Project File No.MoES/ICMAM-PD/ME/CAS-MB/53/2017)

ORCID

M. Sathish  <http://orcid.org/0000-0001-8227-7756>
A. Sundaramanickam  <http://orcid.org/0000-0002-2682-445X>

References

1. Kaur, M.; Rai, J.; Randhawa, G. Recent Advances in Antibacterial Drugs. *Int. J. Appl. Basic Med. Res.* **2013**, 3, 3–10. DOI: [10.4103/2229-516x.112229](https://doi.org/10.4103/2229-516x.112229).
2. Sámano-Valencia, C.; Martínez-Castanon, G. A.; Martínez-Gutiérrez, F.; Ruiz, F.; Toro-Vázquez, J. F.; Morales-Rueda, J. A.; Espinosa-Cristóbal, L. F.; Zavala Alonso, N. V.; Martínez, N. N. Characterization and Biocompatibility of Chitosan Gels with Silver and Gold Nanoparticles. *J. Nanomater.* **2014**, 2014, 1–11. DOI: [10.1155/2014/543419](https://doi.org/10.1155/2014/543419).
3. Sundaramanickam, A.; Suresh Kumar, P.; Kumaresan, S.; Balasubramanian, T. Isolation and Molecular Characterization of Multidrug-Resistant Halophilic Bacteria from Shrimp Farm Effluents of Parangipettai Coastal Waters. *Environ. Sci. Pollut. Res. Int.* **2015**, 22, 11700–11707. DOI: [10.1007/s11356-015-4427-5](https://doi.org/10.1007/s11356-015-4427-5).
4. Filius, P. M. G.; Gyssens, I. C. Impact of Increasing Antimicrobial Resistance on Wound Management. *Am. J. Clin. Dermatol.* **2002**, 3, 1–7. DOI: [10.2165/00128071-200203010-00001](https://doi.org/10.2165/00128071-200203010-00001).
5. Dahal, R. H.; Chaudhary, D. K. Microbial Infections and Antimicrobial Resistance in Nepal: Current Trends and Recommendations. *TOMICROJ* **2018**, 12, 230–242. DOI: [10.2174/1874285801812010230](https://doi.org/10.2174/1874285801812010230).
6. Roberts, C. D.; Leaper, D. J.; Assadian, O. The Role of Topical Antiseptic Agents within Antimicrobial Stewardship Strategies for Prevention and Treatment of Surgical Site and Chronic Open Wound Infection. *Adv. Wound Care* **2017**, 6, 63–71. DOI: [10.1089/wound.2016.0701](https://doi.org/10.1089/wound.2016.0701).
7. Saghaazadeh, S.; Rinoldi, C.; Schot, M.; Kashaf, S. S.; Sharifi, F.; Jalilian, E.; Nuutila, K.; Giatsidis, G.; Mostafalu, P.; Derakhshandeh, H.; et al. Drug Delivery Systems and Materials for Wound Healing Applications. *Adv. Drug Deliv. Rev.* **2018**, 127, 138–166. DOI: [10.1016/j.addr.2018.04.008](https://doi.org/10.1016/j.addr.2018.04.008).
8. Seliktar, D. Designing Cell-Compatible Hydrogels for Biomedical Applications. *Science* **2012**, 336, 1124–1128. DOI: [10.1126/science.1214804](https://doi.org/10.1126/science.1214804).
9. Hoffman, A. S. Hydrogels for Biomedical Applications. *Adv. Drug Deliv. Rev.* **2012**, 64, 18–23. DOI: [10.1016/j.addr.2012.09.010](https://doi.org/10.1016/j.addr.2012.09.010).
10. Saul, J. M.; Williams, D. F. Hydrogels in Regenerative Medicine. In *Handbook of Polymer Applications in Medicine and Medical Devices*; Elsevier: New York, **2013**, pp 279–302.
11. Anitha, A.; Sowmya, S.; Kumar, P. T. S.; Deepthi, S.; Chennazhi, K. P.; Ehrlich, H.; Tsurkan, M.; Jayakumar, R. Chitin and Chitosan in Selected Biomedical Applications. *Prog. Polym. Sci.* **2014**, 39, 1644–1667. DOI: [10.1016/j.progpolymsci.2014.02.008](https://doi.org/10.1016/j.progpolymsci.2014.02.008).
12. Yegappan, R.; Selvaprithiviraj, V.; Amirthalingam, S.; Jayakumar, R. Carrageenan Based Hydrogels for Drug Delivery, Tissue Engineering and Wound Healing. *Carbohydr. Polym.* **2018**, 198, 385–400. DOI: [10.1016/j.carbpol.2018.06.086](https://doi.org/10.1016/j.carbpol.2018.06.086).
13. Kamoun, E. A.; Kenawy, E. R. S.; Chen, X. A Review on Polymeric Hydrogel Membranes for Wound Dressing Applications: PVA-Based Hydrogel Dressings. *J. Adv. Res.* **2017**, 8, 217–233. DOI: [10.1016/j.jare.2017.01.005](https://doi.org/10.1016/j.jare.2017.01.005).
14. Kanmani, P.; Rhim, J. W. Properties and Characterization of Bionanocomposite Films Prepared with Various Biopolymers and ZnO Nanoparticles. *Carbohydr. Polym.* **2014**, 106, 190–199. DOI: [10.1016/j.carbpol.2014.02.007](https://doi.org/10.1016/j.carbpol.2014.02.007).
15. Shankar, S.; Teng, X.; Li, G.; Rhim, J. W. Preparation, Characterization, and Antimicrobial Activity of Gelatin/ZnO Nanocomposite Films. *Food Hydrocoll.* **2015**, 45, 264–271. DOI: [10.1016/j.foodhyd.2014.12.001](https://doi.org/10.1016/j.foodhyd.2014.12.001).
16. Shankar, S.; Rhim, J. W. Effect of Copper Salts and Reducing Agents on Characteristics and Antimicrobial Activity of Copper Nanoparticles. *Mater. Lett.* **2014**, 132, 307–311. DOI: [10.1016/j.matlet.2014.06.014](https://doi.org/10.1016/j.matlet.2014.06.014).
17. Oun, A. A.; Rhim, J. W. Carrageenan-Based Hydrogels and Films: Effect of ZnO and CuO Nanoparticles on the Physical,

- Mechanical, and Antimicrobial Properties. *Food Hydrocoll.* **2017**, 67, 45–53. DOI: [10.1016/j.foodhyd.2016.12.040](https://doi.org/10.1016/j.foodhyd.2016.12.040).
18. Prabhu, Y. T.; Venkateswara Rao, K.; Sessa Sai, V.; Pavani, T. A Facile Biosynthesis of Copper Nanoparticles: A Micro-Structural and Antibacterial Activity Investigation. *J. Saudi Chem. Soc.* **2017**, 21, 180–185. DOI: [10.1016/j.jscs.2015.04.002](https://doi.org/10.1016/j.jscs.2015.04.002).
 19. Chen, X.; Han, W.; Zhao, X.; Tang, W.; Wang, F. Epirubicin-Loaded Marine Carrageenan Oligosaccharide Capped Gold Nanoparticle System for pH-Triggered Anticancer Drug Release. *Sci. Rep.* **2019**, 9, 1–10. DOI: [10.1038/s41598-019-43106-9](https://doi.org/10.1038/s41598-019-43106-9).
 20. Zia, K. M.; Tabasum, S.; Nasif, M.; Sultan, N.; Aslam, N.; Noreen, A.; Zuber, M. A Review on Synthesis, Properties and Applications of Natural Polymer Based Carrageenan Blends and Composites. *Int. J. Biol. Macromol.* **2017**, 96, 282–301. DOI: [10.1016/j.ijbiomac.2016.11.095](https://doi.org/10.1016/j.ijbiomac.2016.11.095).
 21. Salata, O. V. Applications of Nanoparticles in Biology and Medicine. *J. Nanobiotechnol.* **2004**, 2, 3. DOI: [10.1186/1477-3155-2-3](https://doi.org/10.1186/1477-3155-2-3).
 22. Venkatasubbu, G. D.; Baskar, R.; Anusuya, T.; Seshan, C. A.; Chelliah, R. Toxicity Mechanism of Titanium Dioxide and Zinc Oxide Nanoparticles against Food Pathogens. *Colloids Surf. B. Biointerfaces* **2016**, 148, 600–606. DOI: [10.1016/j.colsurfb.2016.09.042](https://doi.org/10.1016/j.colsurfb.2016.09.042).
 23. Saravanakkumar, D.; Oualid, H. A.; Brahmi, Y.; Ayeshamariam, A.; Karunanithy, M.; Saleem, A. M.; Kaviyarasu, K.; Sivarajani, S.; Jayachandran, M. Synthesis and Characterization of CuO/ZnO/CNTs Thin Films on Copper Substrate and Its Photocatalytic Applications. *Open Na* **2019**, 4, 100025. DOI: [10.1016/j.onano.2018.11.001](https://doi.org/10.1016/j.onano.2018.11.001).
 24. Kaviyarasu, K.; Magdalane, C. M.; Kanimozhi, K.; Kennedy, J.; Siddhardha, B.; Subba Reddy, E.; Rotte, N. K.; Sharma, C. S.; Thema, F. T.; Letsholathebe, D.; et al. Elucidation of Photocatalysis, Photoluminescence and Antibacterial Studies of ZnO Thin Films by Spin Coating Method. *J. Photochem. Photobiol. B.* **2017**, 173, 466–475. DOI: [10.1016/j.jphotobiol.2017.06.026](https://doi.org/10.1016/j.jphotobiol.2017.06.026).
 25. Kanimozhi, K.; Khaleel Basha, S.; Sugantha Kumari, V.; Kaviyarasu, K.; Maaza, M. In Vitro Cytocompatibility of Chitosan/PVA/Methylcellulose – Nanocellulose Nanocomposites Scaffolds Using L929 Fibroblast Cells. *Appl. Surf. Sci.* **2018**, 449, 574–583. DOI: [10.1016/j.apsusc.2017.11.197](https://doi.org/10.1016/j.apsusc.2017.11.197).
 26. Mobeen Amanulla, A.; Jasmine Shahina, S. K.; Sundaram, R.; Magdalane, C. M.; Kaviyarasu, K.; Letsholathebe, D.; Mohamed, S. B.; Kennedy, J.; Maaza, M. Antibacterial, Magnetic, Optical and Humidity Sensor Studies of β -CoMoO₄ - Co₃O₄ Nanocomposites and Its Synthesis and Characterization. *J. Photochem. Photobiol. B.* **2018**, 183, 233–241. DOI: [10.1016/j.jphotobiol.2018.04.034](https://doi.org/10.1016/j.jphotobiol.2018.04.034).
 27. Kołodziejczak-Radzimska, A.; Jesionowski, T. Zinc Oxide-from Synthesis to Application: A Review. *Materials (Basel)* **2014**, 7, 2833–2881. DOI: [10.3390/ma7042833](https://doi.org/10.3390/ma7042833).
 28. Roopan, S. M.; Mathew, R. S.; Mahesh, S. S.; Titus, D.; Aggarwal, K.; Bhatia, N.; Damodharan, K. I.; Elumalai, K.; Samuel, J. J. Environmental Friendly Synthesis of Zinc Oxide Nanoparticles and Estimation of Its Larvicidal Activity against *Aedes aegypti*. *Int. J. Environ. Sci. Technol.* **2019**, 16, 8053–8060. DOI: [10.1007/s13762-018-2175-z](https://doi.org/10.1007/s13762-018-2175-z).
 29. Kalaiselvi, A.; Roopan, S. M.; Madhumitha, G.; Ramalingam, C.; Al Dhabbi, N. A.; Arasu, M. V. Catharanthus Roseus-Mediated Zinc Oxide Nanoparticles against Photocatalytic Application of Phenol Red under UV@ 365 nm. *Curr. Sci.* **2016**, 111, 1811–1815. DOI: [10.18520/cs/v111/i11/1811-1815](https://doi.org/10.18520/cs/v111/i11/1811-1815).
 30. Khalid, A.; Khan, R.; Ul-Islam, M.; Khan, T.; Wahid, F. Bacterial Cellulose-Zinc Oxide Nanocomposites as a Novel Dressing System for Burn Wounds. *Carbohydr. Polym.* **2017**, 164, 214–221. DOI: [10.1016/j.carbpol.2017.01.061](https://doi.org/10.1016/j.carbpol.2017.01.061).
 31. Mohandas, A.; Sudheesh Kumar, P. T.; Raja, B.; Lakshmanan, V. K.; Jayakumar, R. Exploration of Alginate Hydrogel/Nano Zinc Oxide Composite Bandages for Infected Wounds. *Int. J. Nanomed.* **2015**, 10, 53–66. DOI: [10.2147/IJN.S79981](https://doi.org/10.2147/IJN.S79981).
 32. Siddiqi, K. S.; Ur Rahman, A.; Tajuddin, Husen, A. Properties of Zinc Oxide Nanoparticles and Their Activity against Microbes. *Nanoscale Res. Lett.* **2018**, 13, 141. DOI: [10.1186/s11671-018-2532-3](https://doi.org/10.1186/s11671-018-2532-3).
 33. Surendra, T. V.; Roopan, S. M.; Al-Dhabbi, N. A.; Arasu, M. V.; Sarkar, G.; Suthindhiran, K. Vegetable Peel Waste for the Production of ZnO Nanoparticles and Its Toxicological Efficiency, Antifungal, Hemolytic, and Antibacterial Activities. *Nanoscale Res. Lett.* **2016**, 11, 546. DOI: [10.1186/s11671-016-1750-9](https://doi.org/10.1186/s11671-016-1750-9).
 34. Jayappa, M. D.; Ramaiah, C. K.; Kumar, M. A. P.; Suresh, D.; Prabhu, A.; Devasya, R. P.; Sheikh, S. Green Synthesis of Zinc Oxide Nanoparticles from the Leaf, Stem and in Vitro Grown Callus of *Mussaenda Frondosa* L.: Characterization and Their Applications. *Appl. Nanosci.* **2020**, 10, 3057–3074. DOI: [10.1007/s13204-020-01382-2](https://doi.org/10.1007/s13204-020-01382-2).
 35. Roopan, S. M.; Nawaz Khan, F. R. ZnO Nanoparticles in the Synthesis of AB Ring Core of Camptothecin. *Chem. Pap.* **2010**, 64, 812–817. DOI: [10.2478/s11696-010-0058-y](https://doi.org/10.2478/s11696-010-0058-y).
 36. Roopan, S. M.; Khan, F. R. N. ZnO Nanorods Catalyzed N-Alkylation of Piperidin-4-One, 4(3H)-Pyrimidone, and Ethyl 6-Chloro-1,2-Dihydro-2-Oxo-4-Phenylquinoline-3-Carboxylate. *Chem. Pap.* **2010**, 64, 678–682. DOI: [10.2478/s11696-010-0045-3](https://doi.org/10.2478/s11696-010-0045-3).
 37. Baskar, K.; Anusuya, T.; Venkatasubbu, G. D. Mechanistic Investigation on Microbial Toxicity of Nano Hydroxyapatite on Implant Associated pathogens. *Mater. Sci. Eng. C. Mater. Biol. Appl.* **2017**, 73, 8–14. DOI: [10.1016/j.msec.2016.12.060](https://doi.org/10.1016/j.msec.2016.12.060).
 38. Venkatasubbu, G. D.; Ramasamy, S.; Gaddam, P. R.; Kumar, J. Acute and Subchronic Toxicity Analysis of Surface Modified Paclitaxel Attached Hydroxyapatite and Titanium Dioxide Nanoparticles. *Int. J. Nanomed.* **2015**, 10, 137–148. DOI: [10.2147/IJN.S79991](https://doi.org/10.2147/IJN.S79991).
 39. Venkatasubbu, G. D.; Ramasamy, S.; Reddy, G. P.; Kumar, J. In Vitro and in Vivo Anticancer Activity of Surface Modified Paclitaxel Attached Hydroxyapatite and Titanium Dioxide Nanoparticles. *Biomed. Microdevices* **2013**, 15, 711–726. DOI: [10.1007/s10544-013-9767-7](https://doi.org/10.1007/s10544-013-9767-7).
 40. Venkatasubbu, G. D.; Ramasamy, S.; Avadhani, G. S.; Ramakrishnan, V.; Kumar, J. Surface Modification and Paclitaxel Drug Delivery of Folic Acid Modified Polyethylene Glycol Functionalized Hydroxyapatite Nanoparticles. *Powder Technol.* **2013**, 235, 437–442. DOI: [10.1016/j.powtec.2012.11.003](https://doi.org/10.1016/j.powtec.2012.11.003).
 41. Devanand Venkatasubbu, G.; Ramasamy, S.; Ramakrishnan, V.; Kumar, J. Hydroxyapatite-Alginate Nanocomposite as Drug Delivery Matrix for Sustained Release of Ciprofloxacin. *J. Biomed. Nanotechnol.* **2011**, 7, 759–767. DOI: [10.1166/jbn.2011.1350](https://doi.org/10.1166/jbn.2011.1350).
 42. Venkatasubbu, G. D.; Ramasamy, S.; Avadhani, G. S.; Palanikumar, L.; Kumar, J. Size-mediated cytotoxicity of nanocrystalline titanium dioxide, pure and zinc-doped hydroxyapatite nanoparticles in human hepatoma cells. *J. Nanoparticle Res.* **2012**, 14, 819. DOI: [10.1007/s11051-012-0819-3](https://doi.org/10.1007/s11051-012-0819-3).
 43. Lee, K. Y.; Mooney, D. J. Alginate: Properties and Biomedical Applications. *Prog. Polym. Sci.* **2012**, 37, 106–126. DOI: [10.1016/j.progpolymsci.2011.06.003](https://doi.org/10.1016/j.progpolymsci.2011.06.003).
 44. Varoni, E.; Tschon, M.; Palazzo, B.; Nitti, P.; Martini, L.; Rimondini, L. Agarose Gel as Biomaterial or Scaffold for Implantation Surgery: Characterization, Histological and Histomorphometric Study on Soft Tissue Response. *Connect Tissue Res.* **2012**, 53, 548–554. DOI: [10.3109/03008207.2012.712583](https://doi.org/10.3109/03008207.2012.712583).
 45. Vignesh, S.; Sivashanmugam, A.; Annapoorna, M.; Janarthanan, R.; Subramania, I.; Shantikumar, V. N.; Jayakumar, R. Injectable Deferoxamine Nanoparticles Loaded Chitosan-Hyaluronic Acid Coacervate Hydrogel for Therapeutic Angiogenesis. *Colloids Surf. B. Biointerfaces* **2018**, 161, 129–138. DOI: [10.1016/j.colsurfb.2017.10.033](https://doi.org/10.1016/j.colsurfb.2017.10.033).
 46. Khattak, S.; Wahid, F.; Liu, L. P.; Jia, S. R.; Chu, L. Q.; Xie, Y. Y.; Li, Z. X.; Zhong, C. Applications of Cellulose and Chitin/Chitosan Derivatives and Composites as Antibacterial Materials:

- Current State and Perspectives. *Appl. Microbiol. Biotechnol.* **2019**, *103*, 1989–2006. DOI: [10.1007/s00253-018-09602-0](https://doi.org/10.1007/s00253-018-09602-0).
47. Gupta, N. V.; Shivakumar, H. G. Investigation of Swelling Behavior and Mechanical Properties of a pH-Sensitive Superporous Hydrogel Composite. *Iran. J. Pharm. Res.* **2012**, *11*, 481–493.
 48. Deen, G.; Chua, V. Synthesis and Properties of New “Stimuli” Responsive Nanocomposite Hydrogels Containing Silver Nanoparticles. *Gels* **2015**, *1*, 117–134. DOI: [10.3390/gels1010117](https://doi.org/10.3390/gels1010117).
 49. Nagaich, U.; Gulati, N.; Chauhan, S. Antioxidant and Antibacterial Potential of Silver Nanoparticles: Biogenic Synthesis Utilizing Apple Extract. *J. Pharm.* **2016**, *2016*, 1–8. DOI: [10.1155/2016/7141523](https://doi.org/10.1155/2016/7141523).
 50. Liu, M.; Ao, P.; Zhou, C.; Shen, Y.; Dai, L.; Liu, Z. The Improvement of Hemostatic and Wound Healing Property of Chitosan by Halloysite Nanotubes. *RSC Adv.* **2014**, *4*, 23540–23553. DOI: [10.1039/C4RA02189D](https://doi.org/10.1039/C4RA02189D).
 51. Nguyen, T. D.; Nguyen, T. T.; Ly, K. L.; Tran, A. H.; Nguyen, T. T. N.; Vo, M. T.; Ho, H. M.; Dang, N. T. N.; Vo, V. T.; Nguyen, D. H.; et al. In Vivo Study of the Antibacterial Chitosan/Polyvinyl Alcohol Loaded with Silver Nanoparticle Hydrogel for Wound Healing Applications. *Int. J. Polym. Sci.* **2019**, *2019*, 1–10. DOI: [10.1155/2019/7382717](https://doi.org/10.1155/2019/7382717).
 52. Anjum, A.; Sim, C.-H.; Ng, S.-F. Hydrogels Containing Antibiofilm and Antimicrobial Agents Beneficial for Biofilm-Associated Wound Infection: Formulation Characterizations and in Vitro Study. *AAPS PharmSciTech.* **2018**, *19*, 1219–1230. DOI: [10.1208/s12249-017-0937-4](https://doi.org/10.1208/s12249-017-0937-4).
 53. Xu, Y.; Li, Y.; Chen, Q.; Fu, L.; Tao, L.; Wei, Y. Injectable and Self-Healing Chitosan Hydrogel Based on Imine Bonds: Design and Therapeutic Applications. *Int. J. Mol. Sci.* **2018**, *19*, 2198. DOI: [10.3390/ijms19082198](https://doi.org/10.3390/ijms19082198).
 54. Khoshhesab, Z. M.; Sarfaraz, M.; Asadabad, M. A. Preparation of ZnO Nanostructures by Chemical Precipitation Method. *Synth. React. Inorganic, Met. Nano-Metal Chem.* **2011**, *41*, 814–819. DOI: [10.1080/15533174.2011.591308](https://doi.org/10.1080/15533174.2011.591308).
 55. AbdElhady, M. M. Preparation and Characterization of Chitosan/Zinc Oxide Nanoparticles for Imparting Antimicrobial and UV Protection to Cotton Fabric. *Int. J. Carbohydr. Chem.* **2012**, *2012*, 1–6. DOI: [10.1155/2012/840591](https://doi.org/10.1155/2012/840591).
 56. Ravindra, S.; Mulaba-Bafubandi, A. F.; Rajinikanth, V.; Varaprasad, K.; Narayana Reddy, N.; Mohana Raju, K. Development and Characterization of Curcumin Loaded Silver Nanoparticle Hydrogels for Antibacterial and Drug Delivery Applications. *J. Inorg. Organomet. Polym. Mater.* **2012**, *22*, 1254–1262. DOI: [10.1007/s10904-012-9734-4](https://doi.org/10.1007/s10904-012-9734-4).
 57. Jung, B. O.; Chung, S. J.; Lee, S. B. Preparation and Characterization of Eugenol-Grafted Chitosan Hydrogels and Their Antioxidant Activities. *J. Appl. Polym. Sci.* **2006**, *99*, 3500–3506. DOI: [10.1002/app.22974](https://doi.org/10.1002/app.22974).
 58. Sudheesh Kumar, P. T.; Lakshmanan, V. K.; Anilkumar, T. V.; Ramya, C.; Reshmi, P.; Unnikrishnan, A. G.; Nair, S. V.; Jayakumar, R. Flexible and Microporous Chitosan Hydrogel/ Nano ZnO Composite Bandages for Wound Dressing: In Vitro and in Vivo Evaluation. *ACS Appl. Mater. Interfaces* **2012**, *4*, 2618–2629. DOI: [10.1021/am300292v](https://doi.org/10.1021/am300292v).
 59. Suner, S. S.; Sahiner, M.; Sengel, S. B.; Rees, D. J.; Reed, W. F.; Sahiner, N. Responsive Biopolymer-Based Microgels/Nanogels for Drug Delivery Applications. In: *Stimuli-Responsive Polymeric Nanocarriers for Drug Delivery, Imaging, and Theragnosis*, Vol. 1; Elsevier: New York, **2018**. DOI: [10.1016/b978-0-08-101997-9.00021-7](https://doi.org/10.1016/b978-0-08-101997-9.00021-7).
 60. Barba, B. J. D.; Tranquilan-Aranilla, C.; Abad, L. V. Hemostatic Potential of Natural/Synthetic Polymer Based Hydrogels Crosslinked by Gamma Radiation. *Radiat. Phys. Chem.* **2016**, *118*, 111–113. DOI: [10.1016/j.radphyschem.2015.02.022](https://doi.org/10.1016/j.radphyschem.2015.02.022).
 61. Shi, X.; Irwin, P. L.; Jin, T.; He, Y.; Xie, Y. Antibacterial Activity and Mechanism of Action of Zinc Oxide Nanoparticles against *Campylobacter jejuni*. *Appl. Environ. Microbiol.* **2011**, *77*, 2325–2331. DOI: [10.1128/aem.02149-10](https://doi.org/10.1128/aem.02149-10).
 62. Sirelkhatim, A.; Mahmud, S.; Seeni, A.; Kaus, N. H. M.; Ann, L. C.; Bakhori, S. K. M.; Hasan, H.; Mohamad, D. Review on Zinc Oxide Nanoparticles: Antibacterial Activity and Toxicity Mechanism. *Nanomicro. Lett.* **2015**, *7*, 219–242. DOI: [10.1007/s40820-015-0040-x](https://doi.org/10.1007/s40820-015-0040-x).
 63. Moreira, R.; Chenlo, F.; Torres, M. D.; Silva, C.; Prieto, D. M.; Sousa, A. M. M.; Hilliou, L.; Gonçalves, M. P. Drying Kinetics of Biofilms Obtained from Chestnut Starch and Carrageenan with and without Glycerol. *Dry. Technol.* **2011**, *29*, 1058–1065. DOI: [10.1080/07373937.2011.563000](https://doi.org/10.1080/07373937.2011.563000).
 64. Tambekar, D.; Dahikar, S. Antibacterial Activity of Some Indian Ayurvedic Preparations against Enteric Bacterial Pathogens. *J. Adv. Pharm. Technol. Res.* **2013**, *2*, 24–29. DOI: [10.4103/2231-4040.79801](https://doi.org/10.4103/2231-4040.79801).
 65. Wang, L.; Hu, C.; Shao, L. The Antimicrobial Activity of Nanoparticles: Present Situation and Prospects for the Future. *Int. J. Nanomed.* **2017**, *12*, 1227–1249. DOI: [10.2147/IJN.S121956](https://doi.org/10.2147/IJN.S121956).
 66. Alves, M. M.; Bouchami, O.; Tavares, A.; Córdoba, L.; Santos, C. F.; Miragaia, M.; de Fátima Montemor, M. New Insights into Antibiofilm Effect of a Nanosized ZnO Coating against the Pathogenic Methicillin Resistant *Staphylococcus aureus*. *ACS Appl. Mater. Interfaces* **2017**, *9*, 28157–28167. DOI: [10.1021/acsami.7b02320](https://doi.org/10.1021/acsami.7b02320).
 67. Rajivgandhi, G.; Maruthupandy, M.; Muneeswaran, T.; Anand, M.; Manoharan, N. Antibiofilm Activity of Zinc Oxide Nanosheets (ZnO NSs) Using *Nocardia* sp. GRG1 (KT235640) against MDR Strains of Gram Negative *Proteus mirabilis* and *Escherichia coli*. *Process Biochem.* **2018**, *67*, 8–18. DOI: [10.1016/j.procbio.2018.01.015](https://doi.org/10.1016/j.procbio.2018.01.015).
 68. Hsueh, Y. H.; Ke, W. J.; Te Hsieh, C.; Lin, K. S.; Tzou, D. Y.; Chiang, C. L. ZnO Nanoparticles Affect *Bacillus subtilis* Cell Growth and Biofilm Formation. *PLoS One* **2015**, *10*, e0128457. DOI: [10.1371/journal.pone.0128457](https://doi.org/10.1371/journal.pone.0128457).
 69. Shakerimoghaddam, A.; Ghaemi, E. A.; Jamali, A. Zinc Oxide Nanoparticle Reduced Biofilm Formation and Antigen 43 Expressions in Uropathogenic *Escherichia coli*. *Iran. J. Basic Med. Sci.* **2017**, *20*, 451–456. DOI: [10.22038/ijbms.2017.8589](https://doi.org/10.22038/ijbms.2017.8589).